PAPER

Check for updates

Cross-linked proton-exchange membranes with strongly reduced fuel crossover and increased chemical stability for direct-isopropanol fuel cells

Sebastian Auffarth, [ID] *[ab] Willibald Dafinger,[ab] Julia Mehler,[a] Valeria Ardizzon,[ab] Patrick Preuster, [ID] [a] Peter Wasserscheid, [ID] [ac] Simon Thiele [ID] [ab] and Jochen Kerres [ID] *[ad]

Isopropanol fuel cells offer an attractive way to provide electric energy from a liquid, easily transportable fuel without producing significant amounts of CO_2. The oxidation product acetone can be easily hydrogenated back to isopropanol to close the storage cycle, thereby avoiding the sophisticated handling of fugitive molecular hydrogen. Until now, direct-isopropanol fuel cells (DIFC) usually rely on various perfluorosulfonic acid ionomers, like Nafion, which are costly and have an unfavorable high fluorine content. Additionally, the dissolution of Nafion in isopropanol/acetone/water solutions within respective applications has prevented the long time operation of DIFCs so far. The swelling of those ionomers during operation promotes fuel crossover and reduces the system's overall energy efficiency. This study uses ionic cross-linking of polymer blends to manufacture chemically stable membranes and introduces a new click-like covalent cross-linking strategy for ion exchange polymers. Compared to Nafion XL, the manufactured membranes increase the maximum power density by up to 10%, resist a dissolution stress test up to 84 w% and reduce the detected isopropanol/acetone crossover up to 75/100% during fuel cell operation. Consequently, the material can be considered a major step toward the technical implementation of isopropanol fuel cell technologies.

Introduction

Compared to elemental hydrogen with its very low volumetric energy density of 3 W h L^{-1} at ambient conditions, liquid organic hydrogen carrier (LOHC) systems promise simplified transport and storage properties and CO_2 emission-free energetic use.[1,2] Among the known LOHC systems, secondary alcohol/ketone pairs are particularly interesting due to the unique properties of secondary alcohols in fuel cells: in contrast to primary alcohols, the oxidation of secondary alcohols stops at the ketone level within the fuel cell, thereby producing no CO_2 within the electrochemically relevant current range.[3] The selective oxidation of the widely available isopropanol within a direct isopropanol fuel cell (DIFC) also features a higher open-circuit potential than other primary alcohol fuels.[4,5] The oxidation product acetone can be easily rehydrogenated by various

catalytic processes.[6–8] Therefore, hydrogenation and dehydrogenation of the acetone/isopropanol couple form a closed cycle, allowing to store energy and convert it back into electric energy on demand by a DIFC. In addition, this concept can be combined with more complex LOHC systems to use their higher hydrogen capacities to regenerate isopropanol from acetone *via* transfer hydrogenation (see Fig. 1).[9]

To secure sufficient proton conductivity below 100 °C in a membrane-electrode-assembly (MEA), perfluorosulfonic acid (PFSA) polymers have been the gold standard for more than fifty years. Various Nafion derivates, for example, are used as membrane materials and binder material in catalyst layers for various types of fuel cells.[10,11] Liquid isopropanol dissolves Nafion rapidly, which leads to strongly reduced lifetimes in a liquid DIFC setup. Since water is required for hydration of Nafion to achieve high proton conductivity, decreasing isopropanol concentration with water in a liquid feed is possible. However, when mixed with water, an isopropanol concentration above 2 M is sufficient to dissolve Nafion from the catalyst layer during liquid-phase operation.[12] While a vaporized feed setup does not show these dissolution effects, the decreased volumetric concentration of isopropanol, especially with a humidified carrier gas, and the energetically unfavorable evaporation process reduce the power density and overall energy efficiency.[4]

[a]Forschungszentrum Jülich GmbH, Helmholtz Institute Erlangen-Nürnberg for Renewable Energy (IEK 11), Cauerstr. 1, 91058 Erlangen, Germany. E-mail: s.auffarth@fz-juelich.de; j.kerres@fz-juelich.de

[b]Department of Chemical and Biological Engineering, Friedrich-Alexander-Universität Erlangen-Nürnberg, Egerlandstr. 3, 91058 Erlangen, Germany

[c]Lehrstuhl für Chemische Reaktionstechnik, Friedrich-Alexander-Universität Erlangen-Nürnberg, Egerlandstr. 3, 91058 Erlangen, Germany

[d]Chemical Resource Beneficiation Faculty of Natural Sciences, North-West University, Potchefstroom 2520, South Africa

17208 | *J. Mater. Chem. A*, 2022, **10**, 17208–17216

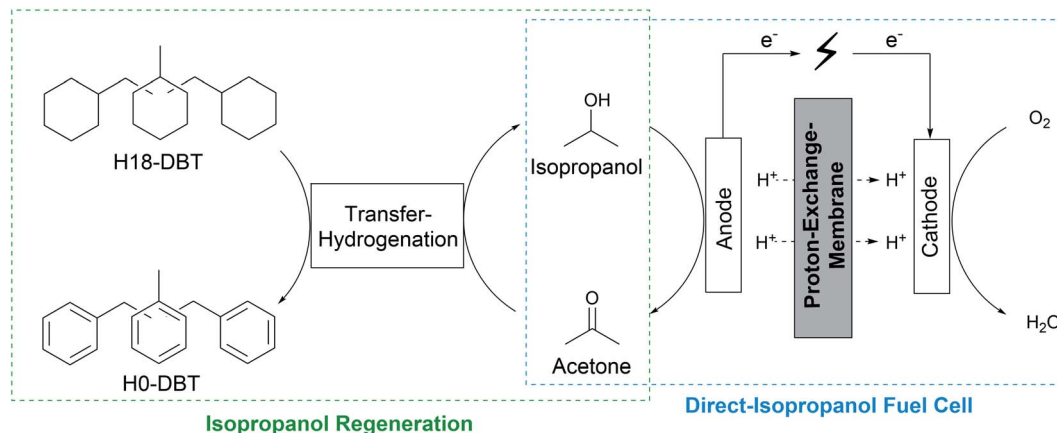This journal is © The Royal Society of Chemistry 2022

Fig. 1 The displayed coupled LOHC system uses hydrogen-rich perhydro dibenzyltoluene (H18-DBT) as a regeneration agent for isopropanol formation *via* transfer hydrogenation. The formed isopropanol is used as fuel for conversion into electrical energy *via* a DIFC. Oxidized acetone can be fully regenerated to isopropanol if neither acetone nor isopropanol is lost due to crossover (closed cycle).

Another problem of DIFCs is the crossover of the isopropanol fuel from the anode to the cathode side through the membrane, which leads to the loss of reactant for proper oxidation, swelling of the MEA and eventually to undesired mixed potentials. The crossover can drastically reduce the performance and overall energy efficiency of the fuel cell.[13] To keep the crossover of isopropanol low, research groups often rely on very thick Nafion membranes (Nafion 117: 183 μm, Nafion 115/105: 127 μm) or Nafion membranes with reinforcement layers and additives (Nafion XL).[4,14–16] Usually, the crossover of isopropanol is measured by linear sweep voltammetry, where the permeated isopropanol is oxidized at the nitrogen-flushed cathode. At the anode-side of the DIFC, protons are reduced to hydrogen, which results in a current proportional to fuel crossover.[4] Fuel crossover depends on many different factors, like operating condition, temperature, fuel concentration, type of used membrane and applied potential.[13] The oxidation product acetone is believed to temporarily block catalyst reaction sites due to slow desorption.[4,5,12,17] Acetone also permeates the membrane, which may lead to unfavorable reaction at the cathode catalyst and acetone loss through the air exhaust of the cell.[4] Lost acetone cannot be regenerated by transfer- or rehydrogenation, thus reducing the sustainability of a closed cycle DIFC operation, as exemplified in Fig. 1.

Several measures are known to address the problem of crossover in fuel cells from the literature. These have been developed mainly for direct methanol fuel cells (DMFC), where the problem of fuel crossover is even more severe than for DIFCs:[5]

- Preparation of Nafion membranes containing SiO_2 nanoparticles[18] or preparation of ZrP nanoparticle-filled Nafion (ZrP = layered zirconium phosphate),[19]
- Use of membranes comprising a Pd barrier layer which suppresses MeOH permeation but allows proton transport,[20]
- Application of fiber mat-reinforced ionomer membranes, such as an electrospun film consisting of Nafion fibers

encapsulated in polyphenylsulfone (PPSU) or of an electrospun membrane consisting of a Nafion film being reinforced by PPSU fibers,[21]

- Use of microporous GoreTex-stretched polytetrafluoroethylene (PTFE) foils as reinforcement layers/materials filled with a Nafion-type PFSA ionomer (GorePrimea membranes),[22,23] or of sulfonated polysulfone (PSU) ionomer embedded in the pores of a stretched PTFE foil,[24]
- Application of covalently cross-linked sulfonated polyether ether ketone (blend-) membranes in which polymer backbone-pendent sulfinate (SO_2Li) groups are covalently cross-linked with α,ω-dihalogenoalkanes by sulfinate S-alkylation.[25–28]

Moreover, ionically cross-linked membranes with different degrees of fluorinated substrates have been developed, which feature a minimized swelling in water–alcohol mixtures and a 37% lower methanol crossover than that of a Nafion 105 membrane at a current density of 100 mA cm^{-2}.[29] Materials with reduced fluorine content require less toxic, environmentally-problematic intermediates compared to the more costly Nafion derivatives.[30,31] Different membrane development approaches for DMFCs have been reviewed.[32]

Due to the similarity between methanol crossover in DMFCs and isopropanol crossover in DIFCs, it is of interest to apply the same strategies for developing improved membranes for direct isopropanol electrification. Besides low fuel crossover, high proton conductivity and chemical stability are additional requirements for a suitable DIFC membrane material. The use of polymer blends allows easy, scalable preparation of membranes from solution casting by combining beneficial properties of different materials.[33]

In this work, we prepared ionically cross-linked membranes and developed a fast approach to establish covalent cross-linking within membranes to overcome the discussed dissolution and crossover issues of PFSA-derivates in DIFCs. The performance and isopropanol crossover of the respective MEAs within DIFC-operation are presented in this contribution.

This journal is © The Royal Society of Chemistry 2022

J. Mater. Chem. A, 2022, **10**, 17208–17216 | **17209**

Experimental

Materials

The polybenzimidazole OPBI (see Fig. 2) with a number/mass average molar mass of $M_n/M_w = 20/24$ kg mol^{-1} was purchased from Fumatech. The polyether SFS (see Fig. 2), $M_n/M_w = 137/296$ kg mol^{-1}, was synthesized according to a literature procedure.[29] All chemicals were used without further purification.

Membrane preparation and crosslinking

SFS was dissolved in dimethylsulfoxide (DMSO, 10 w%), neutralized with nPrNH$_2$ (1.2 eq.), mixed with a DMSO solution of OPBI (5 w%) and stirred until a clear solution was formed. The solution was poured on a glass substrate, doctor bladed to form a thin film and the solvent was evaporated. The membrane was detached in deionized water, post-treated with aqueous sulfuric acid (10 w%) at 85 °C for two days and rinsed with water at 60 °C until neutral pH resulting in the ionically cross-linked membrane A.

For covalent crosslinking, 3,6-dioxa-1,8-octanedithiol (2.5 mol%) was added to a SFS (100 mol%) solution in DMSO (10 w%) and stirred for 10 minutes. Under strong stirring, a 1,8-diazabicyclo[5.4.0]undec-7-ene (DBU) solution in DMSO was added and the reaction mixture was stirred at 70 °C for 20 minutes. A strong viscosity increase was observable within minutes, which indicated covalent cross-linking. Afterward, an OPBI-solution in DMSO (5 w%) was added to the reaction mixture and stirred until a clear solution was formed. The solution was poured on a glass substrate, doctor bladed to form a thin film and the solvent evaporated. The membrane B was detached in deionized water, post-treated with aqueous sulfuric acid (10 w%) at 85 °C for two days and rinsed with water at 60 °C until neutral pH was reached.

To ensure that not all proton-conducting sulfonic groups are ionically cross-linked, the molar polymer ratios in membranes A and B were set to 4.55 : 1 SFS : OPBI. The applied ratios correspond to a theoretical ion-exchange capacity (IEC) of 1.35 mmol g^{-1}.

Membrane characterization

The IECs of membranes A and B were measured by titration using the automated titration processor Omnis from Metrohm, Herisau, Switzerland. Membranes were immersed in a saturated, aqueous NaCl solution to perform an H$^+$/Na$^+$ ion exchange within the membrane for 24 h at 85 °C. The membranes were temporarily removed and the released acid was titrated with 0.1 M NaOH-solution to the equivalent point (calculation of IEC$_{direct}$).

The specific conductivity of all membranes was measured by impedance spectroscopy with a Zennium X from Zahner, Kronach, Germany. The measurements were completed at room temperature and in 0.5 M H$_2$SO$_4$ to minimize contact resistances according to a method described by Kerres et al.[34]

To test the stability of the ionomers against dissolution, dry membranes were immersed in a mixture of isopropanol, acetone and water (v : v : v, 1 : 1 : 1). The respective Schott glasses were sealed and heated up to 85 °C for three days. Potential leftovers of the membrane were removed, dried and weighed. The rest of the solvents were evaporated to gain a potentially dissolved fraction. This fraction was dissolved in deuterated DMSO and analyzed by NMR. To calculate the mass fraction of the leftover membrane, the weight of the dried leftover membrane was divided by the initial dried weight before the stability test. Tests with alternative ketone/alcohol/water mixtures were performed similarly.

The uptake of water and isopropanol was determined by immersing the dry membrane (m_{dry}) in the solvent at 25, 60 and 85 °C. After 24 h the sample was removed, wiped and weighed (m_{wet}). The solvent uptake was determined by dividing the difference $m_{wet} - m_{dry}$ by m_{dry}.

Electrode manufacturing and performance testing

PtRu/C (based on HiSPEC 10000) anodes and Pt/C (based on HiSPEC 4000) cathodes were used for the MEAs. The ink included a 3M ionomer as a binder and was manufactured by doctor-blading onto a Freudenberg gas diffusion layer (GDL). The precise electrode composition is listed in Table 1.

All manufactured MEAs were tested in a fuel cell system from balticFuelCells GmbH with an active area of 4 cm^2. After pre-conditioning with hydrogen, the performance tests with isopropanol were conducted. On the cathode side, the fuel cell was supplied with 1 L$_N$ min^{-1} humidified air (saturated with distilled water at 95 °C). On the anode side, 30 g h^{-1} isopropanol was evaporated and mixed with a humidified nitrogen gas stream (0.5 L$_N$ min^{-1} with 30 g h^{-1} distilled water in a controlled evaporator mixer). The mixture of fuel, water and carrier gas was fed to the fuel cell. All supply lines on the anode and cathode sides were heated to 105 °C. The cell temperature was fixed to 85 °C. The polarization curves were recorded using an electronic load from dhs tools GmbH PLZ164WA.

To investigate the crossover behavior of the manufactured membranes, additional liquid samples were taken. The anode and cathode exhaust gas streams were cooled to condense the organic compounds. The liquid samples were analyzed using a gas chromatograph type Varian 3900 Model OP-8410 with a capillary column and FI detector. The specified crossover is defined as the proportion of component × at the cathode outlet divided by the proportion of component × at the anode outlet.

Results and discussion

Membrane manufacturing and crosslinking

Ionically cross-linked membranes were successfully manufactured according to the literature following a procedure introduced by Schönberger and coworkers.[29] Herein, the basic imidazole groups of the polybenzimidazole OPBI and the acidic sulfonic group of the polyether SFS form an electrostatic interaction between two different polymers (see Fig. 2). Thereby, a network of cross-linked polymer chains is established, which stabilizes the corresponding membrane. Since the protons involved in the ionic cross-links are not available for proton
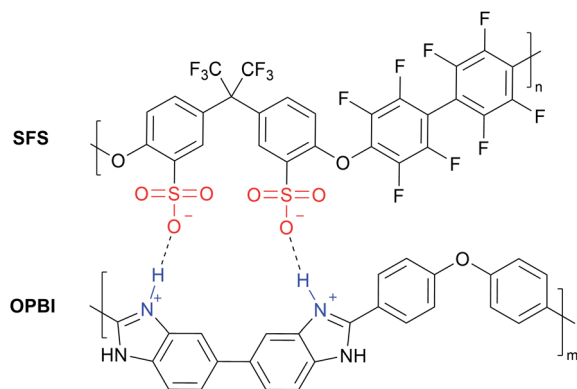
17210 | J. Mater. Chem. A, 2022, 10, 17208–17216

This journal is © The Royal Society of Chemistry 2022

Fig. 2 Ionic cross-linking of OPBI and SFS in membrane A. According to the initially weighed portion, membrane A consists of 82 mol% SFS and 18 mol% OPBI, which results in a theoretical ion exchange capacity (IEC) of 1.35 mmol g^{-1}.

transport, an excess of SFS was used for membrane A to maintain a sufficient proton conductivity.

Since SFS is the proton-conducting polymer and more polar than OPBI, SFS is especially prone to dissolution in polar solvents. To reduce this risk, the SFS chains should be irreversibly connected with a dithiol linker. Terminal thiols can perform nucleophilic substitution reactions at fluorinated aromatic rings like in SFS.[35,36] To activate a thiol for a nucleophilic attack, deprotonation is necessary. To achieve complete activation, a strong base with low nucleophilicity and good solubility in the solvent DMSO is required to deprotonate the weakly acidic thiol cross-linker (pK_a > 9). To obtain covalent cross-linking, the dithiol-3,6-dioxa-1,8-octanedithiol was added to a SFS solution and 1,8-diazabicyclo[5.4.0]undec-7-ene (DBU) was used as the activating base (see Experimental section). An observed viscosity increase of the reaction mixture clearly indicated the onset of successful covalent cross-linking. If an increased amount of a suitable cross-linker is applied, it is also possible to see new emerging signals in ^{19}F-NMR, corresponding to a disubstitution reaction (see Fig. 3). Once the first thiol substitution occurs, the thiol ester activates the opposite side of the fluorinated aromatic ring. This activation phenomenon is already described in the literature and promotes disubstitution.[37,38] By performing an aromatic substitution with a dithiol linker, SFS chains were covalently connected and mixed with OPBI to achieve additional ionic cross-linking after the post-treatment procedure (see Fig. 4). The fast viscosity increase of the reaction mixture can cause manufacturing
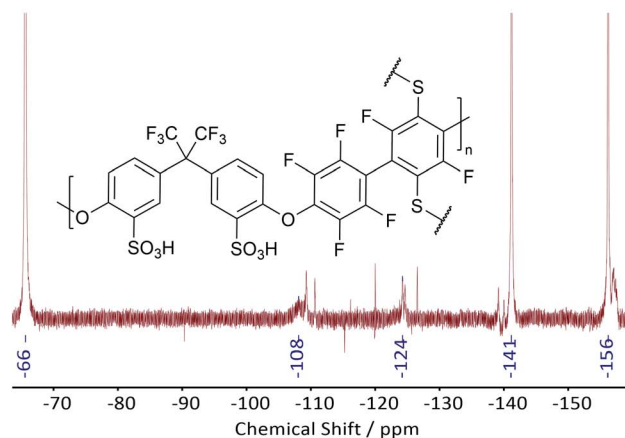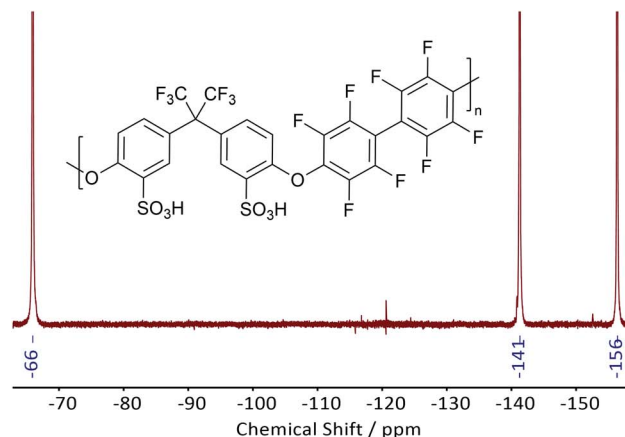

Fig. 3 ^{19}F-NMR of SFS before (top) and after (bottom) the addition of 25 mol% cross-linker. While the spectrum of unfunctionalized SFS (top) only contains peaks at around −66 (−CF$_3$−group), −141 and −156 ppm (both fluorinated biphenyl-group), new peaks at −108 and −124 ppm (both fluorinated biphenyl-group) prove disubstitution at the fluorinated biphenyl-unit of SFS (bottom). The reduced intensity of the completely fluorinated biphenyl group is related to successful nucleophilic substitution. Other peaks may relate to minor mono-substitution and other fluoro-species produced during substitution.

problems that limit the applicable amount of dithiol cross-linker.

Membrane characterization

Table 2 compares thickness, conductivity at room temperature and IEC$_{direct}$ of the ionically cross-linked membrane A and the ionically and covalently cross-linked membrane B. Hauenstein *et al.* achieved the highest power density reported so far for

Table 1 Electrode composition for performance tests

	Anode	Cathode
GDL	Freudenberg H23C4	Freudenberg H14C10
Ionomer to catalyst ratio	0.43	0.43
Catalyst	HiSPEC 10000 (40% Pt, 20% Ru)	HiSPEC 4000 (40% Pt)
Ionomer	3M 725	3M 725
Final loading	1 mg cm^{-2}	0.5 mg cm^{-2}

This journal is © The Royal Society of Chemistry 2022

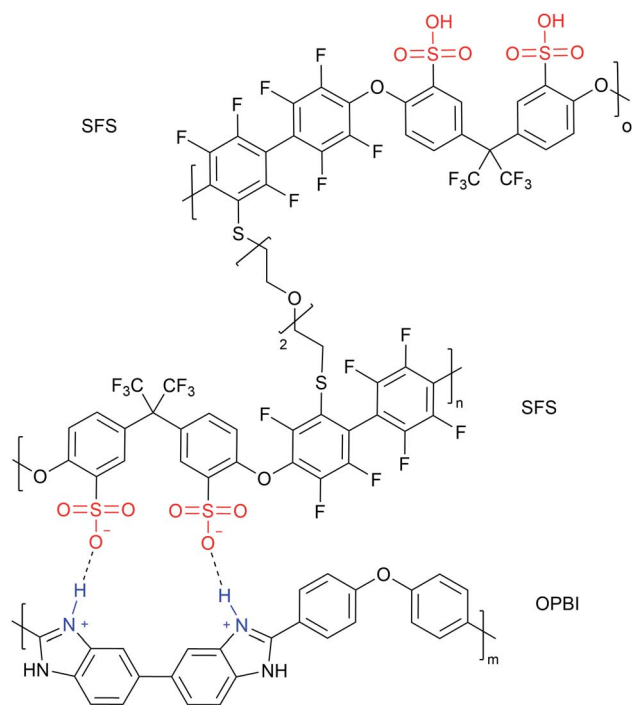*J. Mater. Chem. A*, 2022, **10**, 17208–17216 | **17211**

Fig. 4 Ionic cross-linking of OPBI and SFS with an additional covalent linker between SFS chains in membrane B. According to the initially weighed portion, membrane B consists of 80 mol% SFS, 18 mol% OPBI and 2 mol% cross-linker. This ratio results in a theoretical ion exchange capacity (IEC) of 1.35 mmol g^{-1}.

DIFC with 254 mW cm^{-2} using Nafion XL as the membrane.[15] For our study, comparing pure Nafion membranes without reinforcement is interesting since the here-presented, cross-linked membranes do not have an additional reinforcement layer. Therefore, Nafion XL and Nafion 212 were used as references and comparison materials for further discussions.

First blend membranes of type A possessed a surprisingly low conductivity at room temperature leading to a modest performance in our fuel cell testing. NMR analysis revealed a large amount of residual base from the blending step (triethylamine), which seemed to block the formation of proton-conducting domains within the membrane. Consequently, the more volatile propylamine was used as a neutralizing base during the blending step. The acid post-treatment was performed in sulfuric acid to ensure complete protonation of the sulfonic groups within the membrane. After washing, the

conductivity of the improved membrane of type A increased from 6 mS cm^{-1} to the value of 75 mS cm^{-1} given in Table 2.

While the conductivity at room temperature of Nafion XL was comparable to membrane A, the covalently cross-linked membrane B fell behind in proton conductivity. Although the ratio of basic OPBI to acidic SFS is the same compared to membrane A, the measured IEC_{direct} of membrane B was 0.15 mmol g^{-1} lower. After the post treatment in sulfuric acid, multiple washing steps in water were performed. This washing step removes excess (counter-)ions like SO_4^{2-}, H^+ and $nPrNH_3^+$/DBU-H^+ from the fixed sulfonate anions at the backbone until charge neutrality is achieved. Since H^+ ions are much smaller than $nPrNH_3^+$/DBU-H^+ counterions, those cations (especially DBU-H^+) are less mobile and partly stay within the membrane as counter ions for the sulfonate groups of SFS. These large ions lower the conductivity and the IEC since only H^+ cations account for efficient proton transport. This effect is amplified for membrane B, since DBU is bulkier and less volatile compared to propylamine. Another effect may be that the covalent cross-linker disturbs efficient proton transport next to the sulfonic acid and blocks the removal of bulky DBU during post-treatment.

As expected, the two Nafion membranes dissolved quickly during our harsh solvation testing conditions, as listed in Table 3. The white membrane leftover of Nafion XL was very fragile and lost its initial transparency. From the considerable mass loss which occurred during the stability testing, we concluded that the leftover consists mainly of the insoluble PTFE reinforcement layer and the remaining additives. The proton-conducting PFSA fraction in Nafion XL was thus washed away.

During the stability testing, the ionically cross-linked membrane A maintained its structural properties and showed a considerably lower mass loss than the Nafion membranes. NMR-analysis of the dissolved weight fraction revealed that mainly SFS and the remaining base from the blending step, which was not removed during post-treatment, were dissolved from the membrane. These findings also explain the deviation of the intended IEC of 1.35 mmol g^{-1} to the measured IEC_{direct}. It is likely that the residual base partly blocked the formation of ionic cross-links, allowing SFS to leave the membrane during the stability test more efficiently. The cross-linked membranes could withstand other alcohol/ketone/water mixtures but showed some brownish discoloration, probably caused by residual alcohol within the membrane after testing. The additional covalent cross-linking in membrane B increases the stability against dissolution. According to the literature, the

Table 2 Properties of the membranes manufactured in this work compared to commercial membranes

Tested membranes	Membrane thickness [μm]	Conductivity [mS cm^{-1}]	IEC_{direct} [mmol g^{-1}]
Ionically cross-linked membrane A	57	75 ± 4	1.25
Ionically and covalently cross-linked membrane B	50	37 ± 3	1.10
Nafion 212	50.8[a]	85 ± 7	0.92[a]
Nafion XL	27.5[a]	75 ± 5	—

[a] The data of Nafion 212 and XL were copied from specifications sheets.

17212 | J. Mater. Chem. A, 2022, 10, 17208–17216

This journal is © The Royal Society of Chemistry 2022

Table 3 Results of the dissolution stability testing of different membranes in mixtures (1 : 1 : 1) or pure solvents. Membranes were immersed for three days at 85 °C

Membrane	Test solvents	Mass fraction of leftover membrane (%)
Nafion 212	Water, isopropanol, acetone	0
Nafion XL	Water, isopropanol, acetone	23
Membrane A	Water, isopropanol, acetone	62
Membrane A	Water, 2,5-hexandiol, 2,5-hexandione	62
Membrane A	Water, 2,3-butandiol, 2,3-butandione	66
Membrane A	Pure isopropanol	94
Membrane A	Pure acetone	100
Membrane B	Water, isopropanol, acetone	84
Membrane B	Water, 2,5-hexandiol, 2,5-hexandione	85
Membrane B	Water, 2,3-butandiol, 2,3-butandione	92
Membrane B	Pure isopropanol	98
Membrane B	Pure acetone	101

ethers within the dithiol cross-linker should withstand the acidic conditions applied during fuel cell operation.[10,39–41] The dissolved weight fraction mainly consisted of SFS and residual base from the blending/cross-linking step. However, the amount of residual base determined by NMR was four times higher than for membrane A, probably reducing the conductivity of membrane B. Further stability testing of membrane B in other solvent mixtures confirmed its higher resistance against dissolution compared to membrane A.

The durability of the cross-linked membranes was very high in pure isopropanol and acetone, respectively. Although the difference is not as severe as for the other solvent mixtures, membrane B has higher stability in pure isopropanol. For acetone, the test solvent turned brownish during the stability test, which can be attributed to aldol condensation/addition side reactions of acetone. Some of these side products stayed within the test membranes, which explains the slight mass gain of membrane B during the stability test. While water cannot dissolve the membranes by itself, coordination of water around the ionic cross-links and the acidic groups of the ionomers may be necessary for the partial dissolution of the manufactured membranes in organic solvents. Compared to the Nafion-based membranes, the cross-linked membranes A and B had higher stability against dissolution in solvent mixtures and pure solvents present during DIFC operation.

Since extensive dimensional membrane swelling can cause physical stress on a respective MEA, the uptake of water and isopropanol were determined (see Table 4). At lower temperatures, the lower IEC and the phase separation within the Nafion-based membranes lead to low water uptake. While the cross-linked membranes have a higher water uptake at ambient temperatures, the difference to Nafion 212 diminishes for increased temperatures. This observation also applies to Nafion XL; additives and reinforcements generally help to keep the water uptake at a lower level. Compared to membrane A, the additional covalent cross-links of membrane B reduce water uptake. Since fast proton transport requires sufficient hydration of the sulfonic acid groups, the reduced water uptake of membrane B can be related to the lower conductivity. The uptake of isopropanol for membranes A and B was higher than for water and less dependent on the temperature. The additional covalent cross-linker only reduced the isopropanol uptake of membrane B at ambient temperature. Nafion 212/XL dissolved completely/partly during the immersion in pure isopropanol and no isopropanol uptake was calculated.

DIFC performance and crossover behavior

Since Nafion 212 completely dissolved in the above-mentioned stability test, our performance and crossover tests focused on MEAs using Nafion XL, membrane A and membrane B. Fig. 5 shows the corresponding polarization curves and power densities of the DIFC-performance tests. Fig. 6 shows the acetone, isopropanol and total crossover compared to the maximum power density of the tested membranes.

Similar to Nafion XL, membranes A and B show a s-shaped polarization curve which is characteristic for DIFCs with PtRu catalysts at the anode side.[15] Interestingly, membrane A has been found to outperform Nafion XL in terms of maximum

Table 4 Water and isopropanol uptake of manufactured and reference membranes at different temperatures

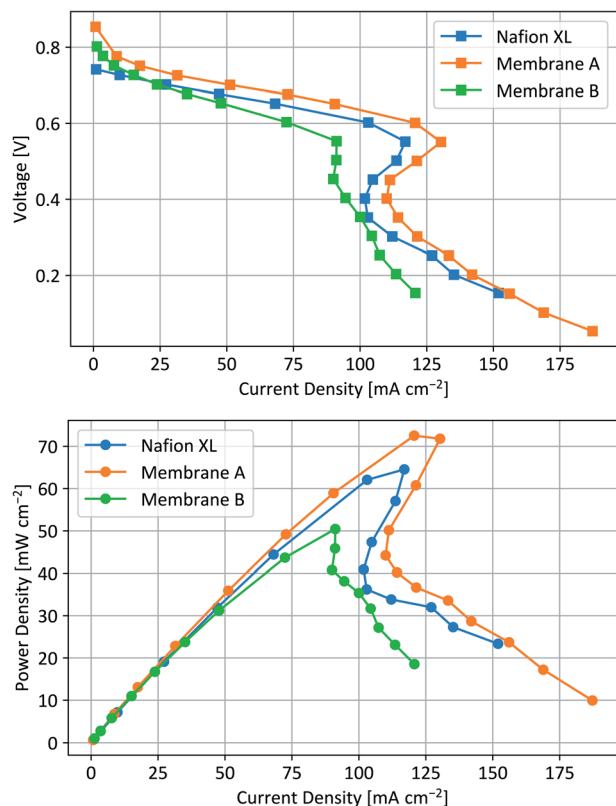|	Water/isopropanol uptake (wt%)		
	25 °C	60 °C	85 °C
Ionically cross-linked membrane A	32/53	39/54	43/57
Ionically and covalently cross-linked membrane B	26/31	30/54	33/53
Nafion 212	16/—	25/—	37/—
Nafion XL	8/—	22/—	27/—

Fig. 5 DIFC–test data of tested MEAs for different membrane materials. Squares represent the polarization curves (top) and circles the power densities (bottom) against the current density.
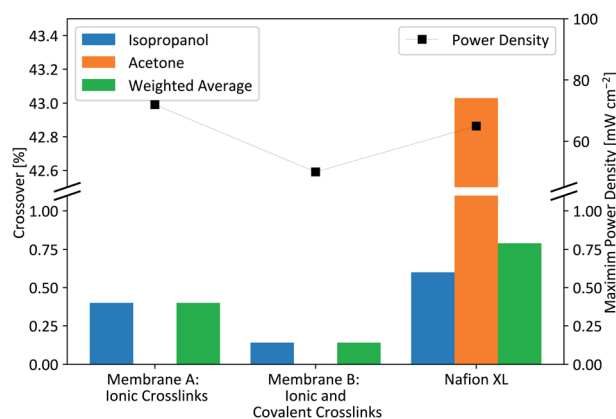

Fig. 6 (Left) Isopropanol and acetone crossover for the tested membranes, (right) maximum power densities of the tested MEAs.

power density, while membrane B showed a slightly lower performance. The decreased power density, the less prominent s-shape and the slightly faster decay in the ohmic region of the polarization curve correspond well with the aforementioned reduced conductivity of membrane B. Although the conductivity of membrane B is only half the value of membrane A, the use of a PFSA-based ionomer in the electrodes and potential interface resistances between electrodes and membrane narrow down the difference in power density. According to the literature,

higher power densities are possible by increasing the catalyst loadings, hot-pressing of MEAs, applying backpressure, or higher cell temperatures.[15] Compared to hydrogen fuel cells, very high catalyst loadings of 4 mg cm^{-2} or higher are often used in literature for DIFC.[4] Since this work focuses on the membrane materials, we refrained from further optimizing the electrodes or the test parameters and kept the maximum catalyst loading at 1 mg cm^{-2}. Both blend membranes A and B have a higher open-circuit voltage (OCV) and a more pronounced activation region than Nafion XL, confirming the lower crossover realized with our novel membrane materials.[42]

No trace of acetone was found at the cathode side by gas chromatography (GC) analysis of the exhaust gas, both for membranes A and B. In contrast, nearly 43% of the produced acetone has been found to permeate through the membrane during fuel cell operation in the case of Nafion XL. Acetone is believed to interact with active catalytic sites through adsorption, decreasing reaction rates.[5,12,17] While it is unclear if the acetone crossover influences the cathodic oxygen reduction reaction, it is obvious that a closed reaction cycle as postulated in Fig. 1 cannot be realized with Nafion XL as a membrane material. In contrast to acetone, the isopropanol crossover using a Nafion XL membrane is only 0.6%. However, the ionically cross-linked membrane A further reduces isopropanol crossover down to 0.4%. Additional covalent cross-linking leads to a further decrease of isopropanol crossover down to 0.15%. While these reductions do not seem to be as significant for vaporized fuel cell operation, the 75% reduction of isopropanol crossover of membrane B can be substantial for long-term and/ or liquid-phase operation. The observed lower OCV in the polarization curve of Nafion XL (compared to membranes A and B) is most likely related to this isopropanol and acetone crossover.

Conclusions

This study presents the benefits of new, fluorine-reduced ionomer blends over the commonly used Nafion materials in DIFC applications, notably suppressing ionomer dissolution and fuel crossover. The blending of acidic and basic aromatic polymers enabled the manufacturing of ionically cross-linked membranes. An aliphatic dithiol was used to covalently cross-link the acidic ionomer chains by a fast click reaction. Conductivity, mechanical properties and IECs of the produced membranes were investigated and found to be very promising. The test of further dithiol cross-linkers appears as an interesting option for future work. The influence of length and composition of the cross-linker may significantly influence the final membrane performance. We anticipate, for example, that the use of aromatic dithiol cross-linkers is attractive as this will reduce the risk of oxidation during preparation by delocalizing the free thiol electron pairs.

Compared to commercial Nafion alternatives, the presented membrane materials of this work successfully withstood complete dissolution in a typical liquid DIFC environment. High stability of membranes against dissolution is crucial for stable fuel cell operation in liquid phase contact. However,

17214 | J. Mater. Chem. A, 2022, 10, 17208–17216

This journal is © The Royal Society of Chemistry 2022

a small weight fraction of the membrane was still lost, indicating that further cross-linking and/or polymer backbone optimizations are necessary. An increased hydrophobicity of the sulfonated polymer would be advantageous for even higher membrane stability. The performance and fuel crossover in DIFC-operation were quantified with MEAs consisting of electrodes with the PFSA-based ionomer from 3M and the manufactured membrane materials. Comparison measurements were performed with a Nafion XL membrane in a similar MEA. Compared to the MEA with Nafion XL, both cross-linked membranes prepared in this work showed a higher OCV with the ionically cross-linked membrane resulting in the highest maximum power density. The lower power density of the MEA with the covalently cross-linked membrane is due to its lower conductivity. In contrast to Nafion XL, the cross-linked membranes ultimately hindered the diffusion of acetone to the cathode. In addition, the cross-linked membranes reduced the isopropanol crossover down to one-fourth of the fuel loss observed for the MEA with Nafion XL.

Since the PFSA-based electrode ionomer is still prone to dissolution, the DIFC-testing performed in this work was still carried out using evaporated isopropanol in a nitrogen gas feed as fuel. Our future work will target the application of cross-linked ionomers, both in the membrane and the electrode, to produce PFSA-free MEAs. Such progress would allow us to operate DIFCs in liquid fuel contact, enabling stable fuel cell operation without vaporization of the isopropanol fuel. For this future research direction, the here-presented cross-linked ionomer blends represent an excellent starting point as they provide high stability against dissolution, superior performance and reduced crossover of fuel and products. In addition, the reduced fluorine content of the new membranes compared to PFSA-derivates, such as Nafion, may help to leverage cost reduction potentials for future CO_2 emission-free, organic fuel cell technologies.

Author contributions

Sebastian Auffarth: conceptualization, methodology, investigation, data curation, visualization, writing – original draft. Willibald Dafinger: methodology, investigation, data curation. Julia Mehler: investigation, data curation. Valeria Ardizzon: methodology. Patrick Preuster: supervision, writing – review & editing, funding acquisition. Peter Wasserscheid: supervision, writing – review & editing, funding acquisition. Simon Thiele: supervision, writing – review & editing, funding acquisition. Jochen Kerres: supervision, conceptualization, writing – review & editing.

Conflicts of interest

There are no conflicts to declare.

Acknowledgements

References

1 P. Preuster, C. Papp and P. Wasserscheid, *Acc. Chem. Res.*, 2017, **50**, 74.

2 D. Teichmann, W. Arlt, P. Wasserscheid and R. Freymann, *Energy Environ. Sci.*, 2011, **4**, 2767.

3 P. Khanipour, F. D. Speck, I. Mangoufis-Giasin, K. J. J. Mayrhofer, S. Cherevko and I. Katsounaros, *ACS Appl. Mater. Interfaces*, 2020, **12**, 33670.

4 M. Brodt, K. Müller, J. Kerres, I. Katsounaros, K. Mayrhofer, P. Preuster, P. Wasserscheid and S. Thiele, *Energy Technol.*, 2021, **9**, 2100164.

5 A. Santasalo, T. Kallio and K. Kontturi, *Platinum Met. Rev.*, 2009, 58.

6 Y. Ji, Y. Wu, G. Zhao, D. Wang, L. Liu, W. He and Y. Li, *Nano Res.*, 2015, **8**, 2706.

7 S. Kishida, *J. Catal.*, 1968, **12**, 90.

8 A. Rahman, *Bull. Chem. React. Eng. Catal.*, 2011, **5**, 113–126, DOI: 10.9767/bcrec.5.2.798.

9 G. Sievi, D. Geburtig, T. Skeledzic, A. Bösmann, P. Preuster, O. Brummel, F. Waidhas, M. A. Montero, P. Khanipour, I. Katsounaros, J. Libuda, K. J. J. Mayrhofer and P. Wasserscheid, *Energy Environ. Sci.*, 2019, **12**, 2305.

10 E. Passalacqua, F. Lufrano, G. Squadrito, A. Patti and L. Giorgi, *Electrochim. Acta*, 2001, **46**, 799.

11 S. Banerjee and D. E. Curtin, *J. Fluorine Chem.*, 2004, **125**, 1211.

12 D. Cao and S. H. Bergens, *J. Power Sources*, 2003, **124**, 12.

13 Z. Qi, *J. Power Sources*, 2002, **112**, 121.

14 D. H. Jung, S. Y. Cho, D. H. Peck, D. R. Shin and J. S. Kim, *J. Power Sources*, 2002, **106**, 173.

15 P. Hauenstein, D. Seeberger, P. Wasserscheid and S. Thiele, *Electrochem. Commun.*, 2020, **118**, 106786.

16 Z. Chen, B. Holmberg, W. Li, X. Wang, W. Deng, R. Munoz and Y. Yan, *Chem. Mater.*, 2006, **18**, 5669.

17 L. D. Burke, *Proc. R. Ir. Acad., Sect. B*, 1989, **89**, 389.

18 A. S. Aricò, P. Cretì, P. L. Antonucci and V. Antonucci, *Electrochem. Solid-State Lett.*, 1998, **1**, 66.

19 C. Yang, S. Srinivasan, A. S. Aricò, P. Cretí, V. Baglio and V. Antonucci, *Electrochem. Solid-State Lett.*, 2001, **4**, A31.

20 C. Pu, W. Huang, K. L. Ley and E. S. Smotkin, *J. Electrochem. Soc.*, 1995, **142**, L119–L120.

21 J. Bryan Ballengee, Electrospun Nanofiber Composite Proton Exchange Membranes, PhD dissertation, Faculty of the Graduate School of Vanderbilt University, Nashville, Tenneessee, 2013.

22 B. Bahar, A. R. Hobson, J. A. Kolde and D. Zuckerbrod, Ultra-Thin Integral Composite Membrane, *US Pat.*, 5547551, 1996.

23 B. Bahar, A. R. Hobson and J. A. Kolde, Integral Composite Membrane, *US Pat.*, 5599614, 1997.

24 S. Mitov, B. Vogel, E. Roduner, H. Zhang, X. Zhu, V. Gogel, L. Jörissen, M. Hein, D. Xing, F. Schönberger and J. Kerres, *Fuel Cells*, 2006, **6**, 413.

25 M. Walker, K.-M. Baumgaertner, M. Kaiser, J. Kerres, A. Ullrich and E. Raeuchle, *J. Appl. Polym. Sci.*, 1999, **74**, 67.

This journal is © The Royal Society of Chemistry 2022

J. Mater. Chem. A, 2022, **10**, 17208–17216 | **17215**

26 W. Zhang, V. Gogel, K. A. Friedrich and J. Kerres, *J. Power Sources*, 2006, **155**, 3.

27 J. Kerres, W. Zhang, L. Jorissen and V. Gogel, *J. New Mater. Electrochem. Syst.*, 2002, **5**, 97.

28 J. Kerres, W. Cui and M. Junginger, *J. Membr. Sci.*, 1998, **139**, 227.

29 F. Schönberger, A. Chromik and J. Kerres, *Polymer*, 2010, **51**, 4299.

30 S. S. Ivanchev, *Russ. J. Appl. Chem.*, 2008, **81**, 569.

31 G. Wei, L. Xu, C. Huang and Y. Wang, *Int. J. Hydrogen Energy*, 2010, **35**, 7778.

32 K. Dutta, P. Kumar, S. Das and P. P. Kundu, *Polym. Rev.*, 2014, **54**, 1.

33 J. A. Kerres, *Polym. Rev.*, 2015, **55**, 273.

34 J. Kerres, A. Ullrich, T. Haering, M. Baldauf, U. Gebhardt and W. Preidel, *J. New Mater. Electrochem. Syst.*, 2000, **3**, 229.

35 G. Delaittre and L. Barner, *Polym. Chem.*, 2018, **9**, 2679.

36 P. M. Imbesi, J. E. Raymond, B. S. Tucker and K. L. Wooley, *J. Mater. Chem.*, 2012, **22**, 19462.

37 C. Langner, J. Meier-Haack, B. Voit and H. Komber, *J. Fluorine Chem.*, 2013, **156**, 314.

38 K. Ninomiya, N. Shida, T. Nishikawa, T. Ishihara, H. Nishiyama, I. Tomita and S. Inagi, *ACS Macro Lett.*, 2020, **9**, 284.

39 B. C. Mei, K. Susumu, I. L. Medintz, J. B. Delehanty, T. J. Mountziaris and H. Mattoussi, *J. Mater. Chem.*, 2008, **18**, 4949.

40 L.-D. Tsai, H.-C. Chien, C.-H. Wang, C.-M. Lai, J.-N. Lin, C.-Y. Zhu and F.-C. Chang, *Int. J. Hydrogen Energy*, 2013, **38**, 11331.

41 C. Lin, R. Thangamuthu and P. Chang, *J. Membr. Sci.*, 2005, **254**, 197.

42 R. P. O'Hayre, S.-W. Cha, W. G. Colella and F. B. Prinz, *Fuel Cell Fundamentals*, Wiley, Hoboken, New Jersey, 2016.

17216 | *J. Mater. Chem. A*, 2022, **10**, 17208–17216

This journal is © The Royal Society of Chemistry 2022